Copyright © 2011 by ABCM

NUMERICAL SIMULATION OF TURBULENT COMBUSTION IN POROUS MATERIALS WITH A TWO ENERGY EQUATION MODEL

José E. A. Coutinho, eduardo@ita.br
Marcelo J. S. de Lemos, delemos@ita.br
Departamento de Energia – IEME
Instituto Tecnológico de Aeronáutica – ITA
12228-900 – São José dos Campos, SP, Brazil

Abstract. *This work presents numerical results for two-dimensional combustion of an air/methane mixture in inert porous media using turbulence and radiation models. Distinct energy equations are considered for the porous burner and for the fuel in it. Inlet velocity and excess air-to-fuel ratio are varied in order to analyze their effects on temperature, turbulent kinetic energy distribution and flame front location. The macroscopic equations for mass, momentum and energy are obtained based on the volume average concept. The numerical technique employed for discretizing the governing equations was the control volume method with a boundary-fitted non-orthogonal coordinate system. The SIMPLE algorithm was used to handle the pressure-velocity coupling. Results indicate that for high excess air values, the gas temperature peak and the turbulent kinetic energy values are reduced. Also, the flame front moves towards the exit of the burner. Results also indicate that the same flame font behavior occurs as we increase the inlet velocity.*

Keywords*: combustion, porous burner, turbulence, radiation*

1. INTRODUCTION

Combustion in inert porous media has been extensively investigated due to the many engineering applications and demand for developing high-efficiency power production devices. The growing use of efficient radiant burners can be encountered in the power and process industries and, as such, proper mathematical models of flow, heat and mass transfer in porous media with combustion can benefit the development of such equipment.

The advantages of having a combustion process inside an inert porous matrix are today well documented in the literature, including basic research for hydrocarbon fuels (Howell *et al.*, 1996), internal combustion engines (Weclas, 2005), lean-combustion porous burners (Wood and Harris, 2008), liquid fuels (Abdul Mujeebu *et al.*, 2009) and a recent view on using hydrogen/air mixtures (Voss *et al.*, 2011) for fuel cell systems. Hsu *et al.* (1993) points out some of its benefits, such as higher burning speed and volumetric energy release rates, higher combustion and flame stability, the ability to burn gases of low energy content, and many other advantages.

Turbulence modeling of combustion within inert porous media has been presented by Lim and Matthews (1998) on the basis of an extension of the standard k - ε model of Jones and Launder (1972).

Motivated by the foregoing, this paper extends the previous works on turbulence modeling in porous media with reactive flows, including numerical simulations using the macroscopic mathematical model proposed by de Lemos (2010a,b). Computations are carried out for inert porous material considering two-dimensional geometry and a two-energy equation model with radiation.

2. MACROSCOPIC MATHEMATICAL MODEL

Equations for turbulent flow in porous media with combustion can be summarized as follows:

2.1. Continuity Equation

$$\nabla \cdot \rho \overline{\mathbf{u}}_D = 0 \tag{1}$$

where $\overline{\mathbf{u}}_D$ is the average surface velocity (also known as seepage, superficial filter or Darcy velocity) and ρ is the fluid density. Equation (1) represents the macroscopic continuity equation for the gas.

2.2. Momentum Equation

$$\nabla \cdot \left(\rho \frac{\overline{\mathbf{u}}_D \overline{\mathbf{u}}_D}{\phi} \right) = -\nabla(\phi \langle \overline{p} \rangle^i) + \mu \nabla^2 \overline{\mathbf{u}}_D + \nabla \cdot \left(-\rho \phi \left\langle \overline{\mathbf{u}'\mathbf{u}'} \right\rangle^i \right) + \phi \rho \mathbf{g} - \left[\frac{\mu \phi}{K} \overline{\mathbf{u}}_D + \frac{c_F \phi \rho |\overline{\mathbf{u}}_D| \, \overline{\mathbf{u}}_D}{\sqrt{K}} \right] \tag{2}$$

where the last two terms in Eq. (2) represent the Darcy and Forchheimer contributions. The symbol K is the porous

medium permeability, $c_F = 0.55$ is the form drag or Forchheimer coefficient, $\langle \overline{p} \rangle^i$ is the intrinsic average pressure of the fluid phase, μ is the fluid dynamic viscosity and ϕ is the porosity of the porous medium.

Turbulence is handled via a macroscopic $k-\varepsilon$ model given by:

$$\nabla \cdot \left(\rho \overline{\mathbf{u}}_D \langle k \rangle^i \right) = \nabla \cdot \left[\left(\mu + \frac{\mu_{t_\varphi}}{\sigma_k} \right) \nabla \left(\phi \langle k \rangle^i \right) \right] - \rho \left\langle \overline{\mathbf{u}'\mathbf{u}'} \right\rangle^i : \nabla \overline{\mathbf{u}}_D + c_k \rho \frac{\phi \langle k \rangle^i |\overline{\mathbf{u}}_D|}{\sqrt{K}} - \rho \phi \langle \varepsilon \rangle^i \tag{3}$$

$$\nabla \cdot \left(\rho \overline{\mathbf{u}}_D \langle \varepsilon \rangle^i \right) = \nabla \cdot \left[\left(\mu + \frac{\mu_{t_\varphi}}{\sigma_\varepsilon} \right) \nabla \left(\phi \langle \varepsilon \rangle^i \right) \right] + c_1 \left(- \rho \left\langle \overline{\mathbf{u}'\mathbf{u}'} \right\rangle^i : \nabla \overline{\mathbf{u}}_D \right) \frac{\langle \varepsilon \rangle^i}{\langle k \rangle^i} + c_2 c_k \rho \frac{\phi \langle \varepsilon \rangle^i |\overline{\mathbf{u}}_D|}{\sqrt{K}} - c_2 \rho \phi \frac{\langle \varepsilon \rangle^{i\,2}}{\langle k \rangle^i} \tag{4}$$

where

$$- \rho \phi \left\langle \overline{\mathbf{u}'\mathbf{u}'} \right\rangle^i = \mu_{t_\varphi} 2 \langle \mathbf{D} \rangle^v - \frac{2}{3} \phi \rho \langle k \rangle^i \mathbf{I} \tag{5}$$

and

$$\mu_{t_\varphi} = \rho c_\mu \frac{\langle k \rangle^{i\,2}}{\langle \varepsilon \rangle^i} \tag{6}$$

Details on the derivation of the above equations can be found in de Lemos (2006).

2.3. Two-Energy Equation Model

When average temperatures in distinct phases are substantially different from each other, for example in combustion processes, macroscopic energy equations are obtained for both fluid and solid phases by applying time and volume average operators to the instantaneous local equations (Saito and de Lemos, 2006). We name this approach Non Local Thermal Equilibrium (NLTE) Model. As in the flow case, volume integration is performed over a Representative Elementary Volume (REV). After including the heat released due the combustion reaction, one gets for both phases:

Gas:

$$\nabla \cdot \left(\rho_f c_{pf} \overline{\mathbf{u}}_D \left\langle \overline{T}_f \right\rangle^i \right) = \nabla \cdot \left\{ \mathbf{K}_{eff,f} \cdot \nabla \left\langle \overline{T}_f \right\rangle^i \right\} + h_i a_i \left(\left\langle \overline{T}_s \right\rangle^i - \left\langle \overline{T}_f \right\rangle^i \right) + \phi \Delta H S_{fu} \tag{7}$$

Solid:

$$0 = \nabla \cdot \left\{ \mathbf{K}_{eff,s} \cdot \nabla \left\langle \overline{T}_s \right\rangle^i \right\} + h_i a_i \left(\left\langle \overline{T}_s \right\rangle^i - \left\langle \overline{T}_f \right\rangle^i \right) \tag{8}$$

where $a_i = A_i / \Delta V$ is the interfacial area per volume unit, h_i is the film coefficient for interfacial transport, $\mathbf{K}_{eff,f}$ and $\mathbf{K}_{eff,s}$ are the effective conductivity tensors for fluid and solid, respectively, given by:

$$\mathbf{K}_{eff,f} = \left\{ \underbrace{\phi\, k_f}_{conduction} \right\} \mathbf{I} + \underbrace{\mathbf{K}_{f,s}}_{local conduction} + \underbrace{\mathbf{K}_{disp}}_{dispersion} + \underbrace{\mathbf{K}_t + \mathbf{K}_{disp,t}}_{turbulence} \tag{9}$$

$$\mathbf{K}_{eff,s} = \left\{ \underbrace{(1-\phi)[k_s}_{conduction} + \underbrace{\frac{16\sigma \left(\langle \overline{T} \rangle^i \right)^3}{3\beta_r}]}_{radiation} \right\} \mathbf{I} + \underbrace{\mathbf{K}_{s,f}}_{local conduction} \tag{10}$$

In Eqs. (7) to (10), $\mathbf{I}$ is the unit tensor, ΔH is the heat of combustion, $\sigma = 5.66961 \times 10^{-8}\ \mathrm{W/m^2K^4}$ is the Stephan-Boltzmann constant, β_r is the extinction coefficient and S_{fu} is the rate of fuel consumption, to be commented bellow.

In Eqs. (9) and (10), all mechanisms contributing to the heat transfer within the medium, together with turbulence and radiation, are here included in order to compare their effect on temperature distribution. Further, such distinct contributions of various mechanisms can be modeled by applying gradient type diffusion expressions, in the form:

Turbulent heat flux:

$$-\left(\rho\, c_p\right)_f\left(\phi\overline{\langle \mathbf{u}'\rangle^i\langle T'_f\rangle^i}\right)=\mathbf{K}_t\cdot\nabla\langle\overline{T}_f\rangle^i \tag{11}$$

Thermal dispersion:

$$-\left(\rho\, c_p\right)_f\left(\phi\langle {}^i\overline{\mathbf{u}}^i\overline{T}_f\rangle^i\right)=\mathbf{K}_{disp}\cdot\nabla\langle\overline{T}_f\rangle^i \tag{12}$$

Turbulent thermal dispersion:

$$-\left(\rho\, c_p\right)_f\left(\phi\langle\overline{{}^i\mathbf{u}'^i T_f}\rangle^i\right)=\mathbf{K}_{disp,t}\cdot\nabla\langle\overline{T}_f\rangle^i \tag{13}$$

Local conduction:

$$\begin{aligned}\nabla\cdot\left[\frac{1}{\Delta V}\int_{A_i}\mathbf{n}_i k_f\overline{T}_f dA\right]&=\mathbf{K}_{f,s}\cdot\nabla\langle\overline{T}_s\rangle^i\\ -\nabla\cdot\left[\frac{1}{\Delta V}\int_{A_i}\mathbf{n}_i k_s\overline{T}_s dA\right]&=\mathbf{K}_{s,f}\cdot\nabla\langle\overline{T}_f\rangle^i\end{aligned} \tag{14}$$

In Eqs. (7) and (8) the heat transferred between the two phases was modeled by means of a film coefficient h_i. A numerical correlation for the interfacial convective heat transfer coefficient was proposed by Kuwahara *et al.* (2001) for laminar flow as:

$$\frac{h_i D}{k_f}=\left(1+\frac{4(1-\phi)}{\phi}\right)+\frac{1}{2}(1-\phi)^{1/2}\,\mathrm{Re}_D\,\mathrm{Pr}^{1/3},\ \text{valid for}\ 0.2<\phi<0.9 \tag{15}$$

For turbulent flow, the following expression was proposed by Saito and de Lemos (2006):

$$\frac{h_i D}{k_f}=0.08\left(\frac{\mathrm{Re}_D}{\phi}\right)^{0.8}\mathrm{Pr}^{1/3};\ \text{for}\ 1.0\times10^4<\frac{\mathrm{Re}_D}{\phi}<2.0\times10^7,\ \text{valid for}\ 0.2<\phi<0.9 \tag{16}$$

2.4. Mass Transport Equation

Transport equation for the fuel reads:

$$\nabla\cdot\left(\rho\overline{\mathbf{u}}_D\langle\overline{m}_{fu}\rangle^i\right)=\nabla\cdot\rho\mathbf{D}_{eff}\cdot\nabla\left(\phi\langle\overline{m}_{fu}\rangle^i\right)-\phi S_{fu} \tag{17}$$

where $\langle\overline{m}_{fu}\rangle^i$ is the mass fraction for the fuel. The effective mass transport tensor $\mathbf{D}_{eff}$ is defined as:

$$\mathbf{D}_{eff}=\underbrace{\mathbf{D}_{disp}}_{dispersion}+\underbrace{\mathbf{D}_{diff}}_{diffusion}+\underbrace{\mathbf{D}_t+\mathbf{D}_{disp,t}}_{turbulence}=\mathbf{D}_{disp}+\frac{1}{\rho}\left(\frac{\mu_\phi}{Sc_\ell}+\frac{\mu_{t_\phi}}{Sc_{\ell,t}}\right)\mathbf{I}=\mathbf{D}_{disp}+\frac{1}{\rho}\left(\frac{\mu_{\phi,ef}}{Sc_{\ell,ef}}\right)\mathbf{I} \tag{18}$$

where Sc_ℓ and $Sc_{\ell,t}$ are the laminar and turbulent Schmidt number for species ℓ, respectively, and "ef" denotes an effective value. The dispersion tensor is defined such that:

$$-\rho_f\phi\langle {}^i\overline{\mathbf{u}}^i\overline{m}_{fu}\rangle^i=\rho_f\mathbf{D}_{disp}\cdot\nabla\left(\phi\langle\overline{m}_{fu}\rangle^i\right) \tag{19}$$

2.4. Simple Chemistry

In this work, for simplicity, the chemical exothermic reaction is assumed to be instantaneous and to occur in a single step, kinetic-controlled, which, for combustion of a mixture air/methane, is given by the chemical reaction (Mohamad *et al.*, 1994a):

$$\mathrm{CH_4} + 2(1+\Psi)(\mathrm{O_2} + 3.76\mathrm{N_2}) \rightarrow \mathrm{CO_2} + 2\mathrm{H_2O} + 2\Psi\,\mathrm{O_2} + 7.52(1+\Psi)\mathrm{N_2} \tag{20}$$

For N-heptane, a similar equation reads (Mohamad *et al.*, 1994b):

$$\mathrm{C_7H_{16}} + 11(1+\Psi)(\mathrm{O_2} + 3.76\mathrm{N_2}) \rightarrow 7\mathrm{CO_2} + 8\mathrm{H_2O} + 11\Psi\,\mathrm{O_2} + 41.36(1+\Psi)\mathrm{N_2} \tag{21}$$

And for Octane, we have:

$$\mathrm{C_8H_{18}} + 12.5(1+\Psi)(\mathrm{O_2} + 3.76\mathrm{N_2}) \rightarrow 8\mathrm{CO_2} + 9\mathrm{H_2O} + 12.5\Psi\,\mathrm{O_2} + 47(1+\Psi)\mathrm{N_2} \tag{22}$$

where Ψ is the excess air in the reactant stream at the inlet of the porous foam. For the stoichiometric ratio, $\Psi = 0$. In all of these equations, the reaction is then assumed to be kinetically controlled and occurring infinitely fast. A general expression for them can be derived as (de Lemos 2010*a,b*):

$$\mathrm{C_nH_{2m}} + \left(\mathrm{n} + \frac{\mathrm{m}}{2}\right)(1+\Psi)(\mathrm{O_2} + 3.76\mathrm{N_2}) \rightarrow \mathrm{nCO_2} + \mathrm{mH_2O} + \left(\mathrm{n} + \frac{\mathrm{m}}{2}\right)\Psi\mathrm{O_2} + \left(\mathrm{n} + \frac{\mathrm{m}}{2}\right)3.76(1+\Psi)\mathrm{N_2} \tag{23}$$

where the coefficients n and m can be found in the Tab. 1. Equation (23) is here assumed to hold for the particular examples given in the table. Here, however, we only apply Eq. (20).

Table 1. Coefficients in the Eq. (23)

Gas	n	m	$(n+m/2)$	$(n+m/2)\times 3.76$
Methane	1	2	2	7.52
N-heptane	7	8	11	41.36
Octane	8	9	12.5	47

The local instantaneous rate of fuel consumption over the total volume (fluid plus solid) was determined by a one-step Arrhenius reaction (Kuo, 2005) given by:

$$S_{fu} = \rho_f^a A m_{fu}^b m_{ox}^c e^{-E/R\langle \bar{T} \rangle^i} \tag{24}$$

where m_{fu} and m_{ox} are the local instantaneous mass fractions for the fuel and oxidant, respectively, and coefficients a, b and c depends on the particular reaction (Kuo, 2005). Here, for simplicity, we assume $a = 2$, $b = c = 1$, which corresponds to the burning of a mixture of methane and air (de Lemos, 2009). Also, in equation (24), A is the pre-exponential factor and E is the activation energy, where numerical values for these parameters depend on the fuel considered (Turns, 2000).

Density ρ_f in the above equation is determined from the perfect gas equation for a mixture of perfect gases:

$$\rho_f = \frac{P_0}{RT_f \sum_1^{\ell} \frac{m_\ell}{M_\ell}} \tag{25}$$

where P_0 is the absolute pressure, $R = 8.134\mathrm{J/(mol.K)}$ is the universal gas constant and M_ℓ is the molecular weight of species ℓ.

3. RESULTS AND DISCUSSION

The problem considered consists in having a porous media confined in a channel, through which a mixture of fuel and air enters from the left, as show in Fig. 1. The fuel/air mixture is injected through an inlet clearance of size less than the burner height., so that flow expansion occurs past the chamber entrance.

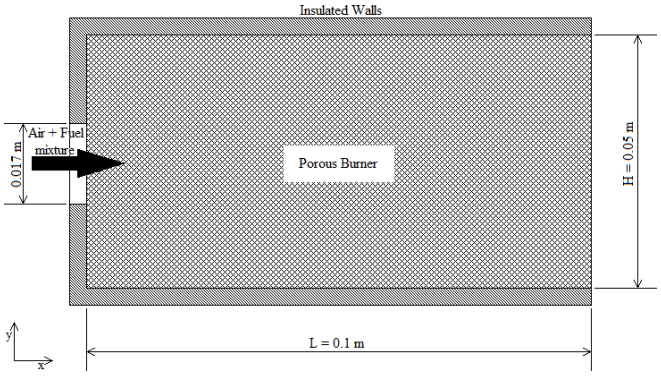

Figure 1 - Two-dimensional combustor model

Simulations assumed given temperatures (solid and gas) and fuel mass fraction at inlet ($x = 0$). At exit ($x = 10$ cm), a zero diffusion condition ($\partial(\ )/\partial x = 0$) for all variables was considered. For the solid temperature, a balance between the energy conducted to the exit of the burner and the radiation leaving the porous material to the environment was applied. Further, the entire burner is made of the same material. For all the cases, the porosity considered was $\phi = 0.8$.

The finite-volume technique was employed to discretize the transport equations. The resulting algebraic equation set was relaxed using the well-known segregate method SIMPLE. Further, the flame front position was calculated during the solution process, related to the heat release rate as show in Eq. (24), so no artificial numerical set-up was implemented for holding the flame at some particular location.

Figure 2 shows the axial temperature profile at the centerline ($y = H/2$) calculated for two different grid sizes, namely 102x52 and 153x78. As we can note in the figure, no significant detectable differences exist between the two sets of results.

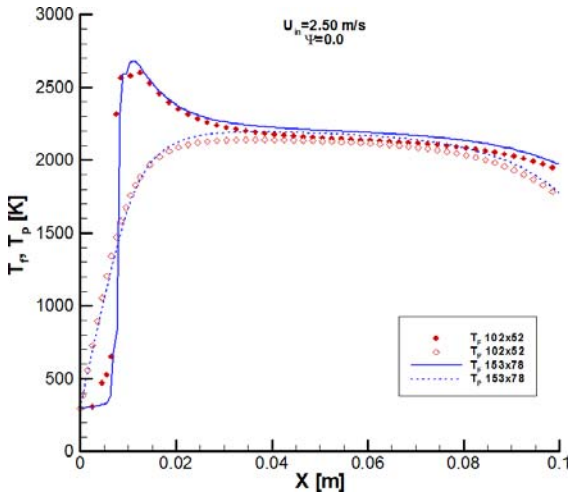

Figure 2
Grid independence study

For this reason, and considering the computational cost (processing time, memory allocation, etc.), all simulations in this paper make use of the 102x52 grid, which is showed on Fig. 3.

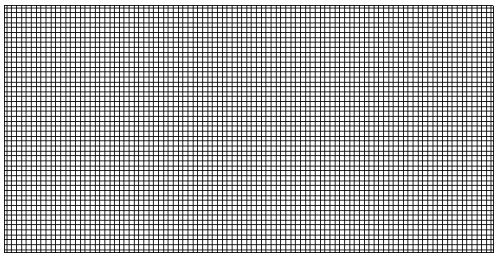

Figure 3 -Computational grid, 102x52 nodes.

Next, we present here two sets of results. The first one considers the effect of the inlet velocity U_{in} on the flame front location and on the temperatures of the fluid and the porous material. They were obtained by maintaining the value of the excess air Ψ constant and varying the value of U_{in} from 0.25 m/s to 5.00 m/s. Three values for the excess air were considered, namely, $\Psi = 0.0$, $\Psi = 0.5$ and $\Psi = 0.8$.

The second set of results investigates the effect of varying Ψ while maintaining the value of U_{in}. The excess air was varied from 0.0 to 0.9 for three values of fixed inlet velocities, namely 1.25 m/s, 2.50 m/s and 5.00 m/s.

Figure 4 shows the effect on the flame front location for the two sets of results. The simulations for leaner mixtures (Figs. 4b,c) show that the flame front is more sensitive to the mass flow rate and that the flame front is pushed towards the exit as we increase the inlet velocity. Although not shown here, for very lean mixtures, the opening of the flame front at higher values of U_{in} occurs, causing the release of unburned fuel to the environment.

Also, as we increase the inlet velocity, the flame front location becomes more sensitive for higher values of Ψ (Figs. 4a',c').

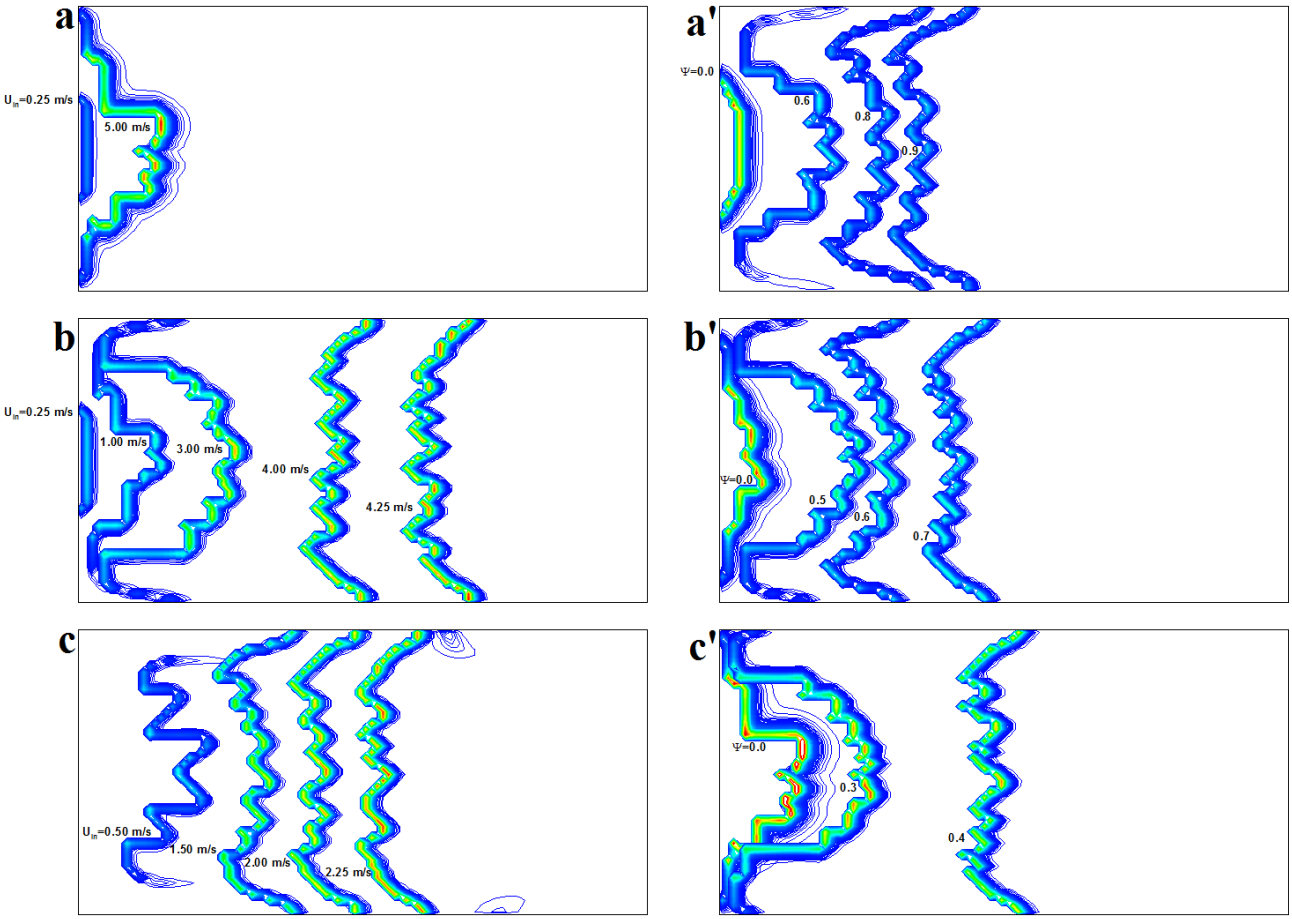

Figure 4 - Flame front location: Effect of excess air, Ψ : **a)** $\Psi = 0.0$, **b)** $\Psi = 0.5$, **c)** $\Psi = 0.8$; effect of inlet velocity U_{in} : **a')** $U_{in} = 1.25\text{m/s}$, **b')** $U_{in} = 2.50\text{m/s}$, **c')** $U_{in} = 5.00\text{m/s}$

Figure 5 shows results for temperatures at the centerline of the burner ($y = H/2$). As we can see in Fig. 5b for $\Psi = 0.5$ and Fig. 5c for $\Psi = 0.8$, minimum variations of the inlet velocity cause great differences on temperatures compared to the stoichiometric case (Fig. 5a). Also, peak temperatures increase as U_{in} is increased. We can also observe that at higher inlet velocities, higher radiation fluxes at the outlet zone are detected.

The effect of the inlet velocity is shown next in Figs. 5a',b',c' for distinct values of Ψ. Also here we can notice that for higher excess air ratios, the temperature peak decreases, regardless of the inlet velocity values. The reduction of the temperature peak is more evident for low values of Ψ. As we increase Ψ, the maximum temperature of the fluid tends to reach a constant value, with a shift on the position of the temperature peak. We can also notice that values close to $\Psi = 0$ have greater radiation heat losses at the exit of the burner. Further, such losses decrease as we increase the excess air.

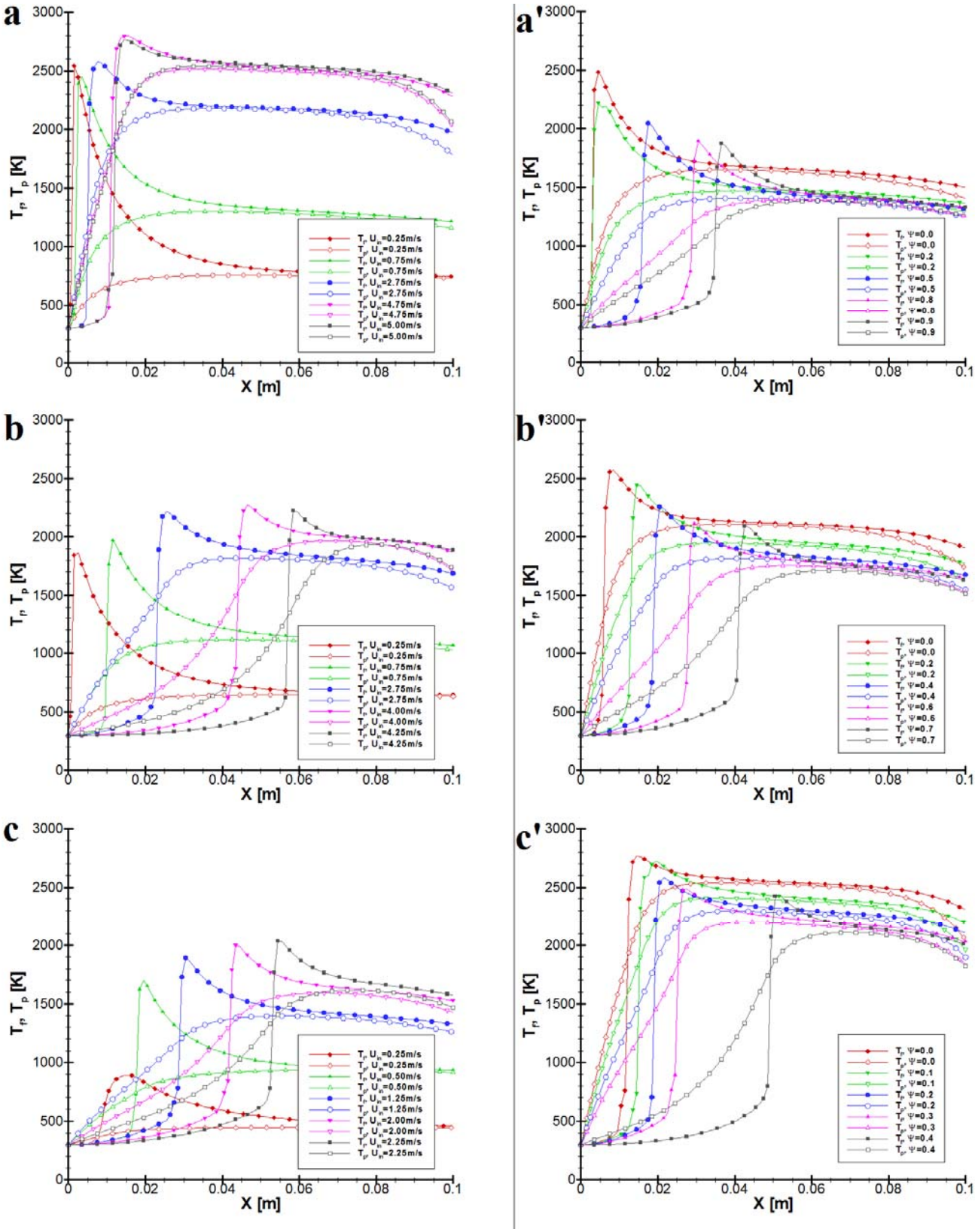

Figure 5 –Axial temperature profiles at $y = H/2$: Effect of air-to-fuel ratio Ψ : **a)** $\Psi = 0.0$, **b)** $\Psi = 0.5$, **c)** $\Psi = 0.8$; effect of inlet velocity U_{in} : **a')** $U_{in} = 1.25\text{m/s}$, **b')** $U_{in} = 2.50\text{m/s}$, **c')** $U_{in} = 5.00\text{m/s}$

Finally, results for the statistical flow field are shown in Fig. 6. As we can see on Figs. 6a, b and c, the turbulent kinetic energy (k) present a similar behavior when compared to the temperature distribution (see Fig. 5). Maintaining a constant value of Ψ , as we increase the inlet velocity, the value of k increases as well. As the mixture becomes leaner (Figs. 6b, c), we can observe that minimum variations of U_{in} gives rise to large relative variations on the turbulent kinetic energy.

Also, for a constant inlet velocity (Figs. 6a',b',c'), greatest values of k occurs when the mixture approaches the stoichiometric condition. As we increase Ψ, variations of turbulent kinetic energy levels are minimized. The location of the maximum value of k seems to correspond to temperature peak locations (see Fig. 5).

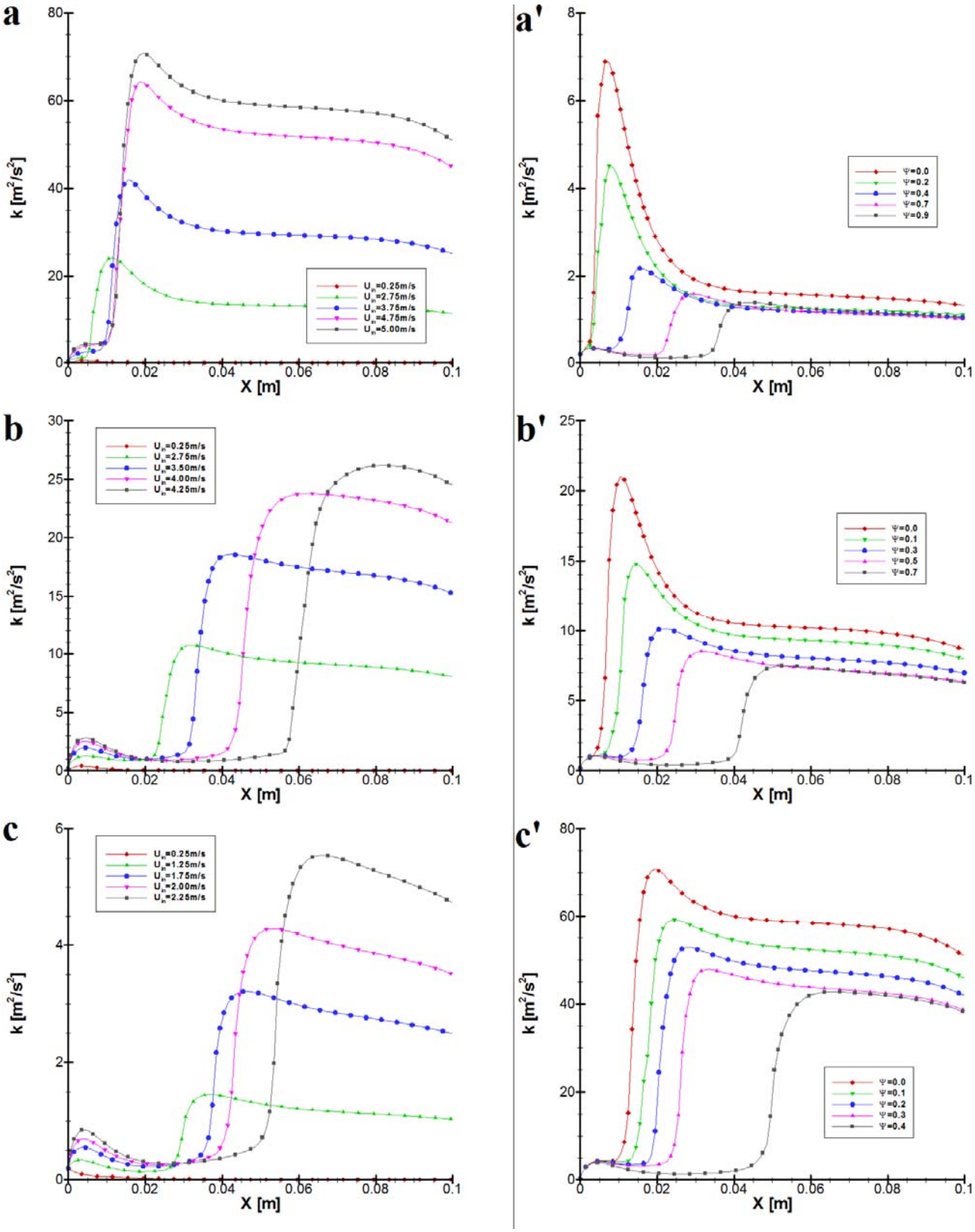

Figure 6 – Axial turbulent kinetic energy profiles at $y=H/2$. Effect of excess air Ψ : **a**) $\Psi = 0.0$, **b**) $\Psi = 0.5$, **c**) $\Psi = 0.8$; effect of inlet velocity U_{in} : **a'**) $U_{in} = 1.25\text{m/s}$, **b'**) $U_{in} = 2.50\text{m/s}$, **c'**) $U_{in} = 5.00\text{m/s}$.

4. CONCLUSIONS

This work presented two-dimensional simulations for a mixture of air and methane burning in a porous material. Simulations presented made use of the NLTE model, using further mathematical models for turbulence and radiation transport. Results indicate that for high excess air, the flame moves towards the exit of the burner. This effect is also observed for higher inlet velocities. Additional research work on the subject of modeling reactive turbulent flow in porous burners is needed in order to validate the preliminary results shown in this work. Results herein should, therefore, be seen as a first step towards reliable simulation of real porous combustors.

5. ACKNOWLEDGEMENTS

The authors are thankful to CNPq, Brazil, for their financial support during the course of this research at LCFT-ITA.

6. REFERENCES

Abdul Mujeebu, M., Abdullah, M.Z., Abu Bakar,M.Z., Mohamad, A.A., Abdullah, M.K., 2009a, "A review of investigations on liquid fuel combustion in porous inert media", Progress in Energy and Combustion Science, Vol.35, pp. 216-230

de Lemos, M.J.S., 2006, “Turbulence in Porous Media: Modeling and Applications”, Elsevier, Amsterdam, Netherlands, 384 p.

de Lemos, M.J.S., 2009, “Numerical Simulation of Turbulent Combustion in Porous Materials”, International Communications in Heat and Mass Transfer, Vol.36, pp. 996-1001

de Lemos, M.J.S., 2010a, "Analysis of turbulent combustion in inert porous media", International Communications in Heat and Mass Transfer, Vol.37, pp. 331-336

de Lemos, M.J.S.. 2010b, Simulation of Turbulent Combustion in Porous Materials with One- and Two-Energy Equations Models. In: Oechsner, A., Murch, G.E.. (Org.). Chapter 16 in: Heat Transfer in Multi-Phase Materials. Berlin: Springer, 2010, v. 2, p. 1-30.

Howell, J.R., Hall, M.J., Ellzey, J.L., 1996, "Combustion of Hydrocarbon Fuels within Porous Inert Media", Progress in Energy and Combustion Science, Vol.122, pp. 121-145

Hsu, P.-F, Howell, J.R., Matthews, R.D., 1993, "A Numerical Investigation of Premixed Combustion within Porous Inert Media", Journal of Heat Transfer, Vol.115, pp. 744-750

Jones, W.P., Launder, B.E, 1972, "The Prediction of Laminarization with a Two-equation Model of Turbulence", International Journal of Heat and Mass Transfer, Vol.15, pp. 301-314

Kuo, K. K., 2005, “Principles of Combustion”, Second Edition, John Wiley & Sons, New Jersey, USA, 760 p.

Kuwahara, F., Shirota, M., Nakayama, A., 2001, “A Numerical Study of Interfacial Convective Heat Transfer Coefficient in Two-Energy Equation Model for Convection in Porous Media”, International Journal of Heat and Mass Transfer, Vol.44, pp. 1153-1159

Lim, I.-G., Matthews, R.D., 1998, "Development of a Model for Turbulent Combustion, within Porous Inert Media", International Journal of Fluid Mechanics Research, Vol. 25, Nos.1-3, pp. 111-122

Mohamad, A. A., Ramadhyani, S., Viskanta, R., 1994a, “Modeling of Combustion and Heat-Transfer in a Packed-Bed with Embedded Coolant Tubes”, International Journal of Heat and Mass Transfer, Vol.37, Issue 8, pp. 1181-1191

Mohamad, A. A., Viskanta, R., Ramadhyani, S., 1994b, “Numerical Prediction of Combustion and Heat Transfer in a Packed Bed with Embedded Coolant Tubes”, Combustion Science and Technology, Vol. 96, pp. 387-407

Peard, T. E., Peters, J. E., Brewster, B., Buckius, R. O., 1993, “Radiative Heat Transfer Augmentation in Gas-Fired Radiant Tube Burnerby Porous Inserts: Effect on Insert Geometry”, Experimental Heat Transfer, Vol.6, pp. 273-286

Saito, M. B., de Lemos, M. J. S., 2006, “A Correlation for Interfacial Heat Transfer Coefficient for Turbulent Flow over an Array of Square Rods”, Journal of Heat Transfer, Vol.128, pp. 444-452

Turns, S. R., 2000, “An Introduction to Combustion: Concepts and Applications”, Second Edition, McGraw-Hill, New York, USA, 704 p.

Voss, S., Steinbrück, R., Kautz, M., Schießwohl, E., Arendt, M., Felde, J.T., Volkert, J., Trimis, D., 2011, "Premixed hydrogen-air combustion system for fuel cell systems", International Journal of Hydrogen Energy, Vol.36, pp. 3697-3703

Weclas M., 2005, "Potential of porous medium combustion technology as applied to internal combustion engines", Sonderdruck Schriftenreihe University of Applied Sciences in Nürnberg, Vol.32., pp.1–24.

Wood, S., Harris, A.T., 2008, "Porous burners for lean-burn applications", Progress in Energy and Combustion Science, Vol.34, pp. 667-684

7. RESPONSIBILITY NOTICE

The authors are the only responsible for the printed material included in this paper.